Layer-Specific Manganese-Enhanced MRI of the Retina in Light and Dark Adaptation

Bryan H. De La Garza,[1] *Guang Li,*[1] *Yen-Yu I. Shih,*[1] *and Timothy Q. Duong*[1-3]

Purpose. To employ functional manganese-enhanced MRI (MEMRI) to image layer-specific changes in calcium-dependent activities in the rat retina during light versus dark adaptation.

Methods. Functional MEMRI at $20 \times 20 \times 700$ μm was used to study light and dark adaptation in the same animals ($N = 10$) in which one eye was covered and the fellow eye was not. The activity encoding of the light and dark adaptation was achieved in awake conditions and imaged under anesthesia. T_1-weighted MRI at 11.7 tesla (T) was performed using two identical radiofrequency transceiver coils to allow interleaved MRI acquisitions of the two eyes. An intravascular contrast agent was also used to verify layer assignments.

Results. MEMRI detected contrasts among the inner retina, outer retina, and choroid. Independent confirmation of the vascular layers and boundaries between layers was documented with an intravascular contrast agent. The retinal layer thicknesses agreed with published data. The outer retina had lower MEMRI activity in light compared with dark adaption ($P < 0.001$), consistent with the increased metabolic demand associated with the "dark current." The inner retina had higher MEMRI activity in light compared with dark adaption ($P < 0.05$). The choroid MEMRI activity was not statistically different between light and dark adaptation ($P > 0.05$).

Conclusions. This study demonstrated a high-resolution MEMRI protocol to image functional activities among different layers of the retinas in awake animals during light and dark adaptation. This approach could have potential applications in animal models of retinal dysfunction. (*Invest Ophthalmol Vis Sci.* 2012;53:4352–4358) DOI:10.1167/iovs.11-8826

Light and dark adaptation of the retina remains of significant interest. Oxygen tension, electrical activity and oxygen and glucose consumption, and blood flow have been reported associated with light and dark adaptation (see review[1]). There is consensus that the neuronal activity in the outer retina increases in dark relative to light. Choroid blood flow, which predominantly supplies the outer retina, does not differ between light and dark,[2] although exception has been noted.[3] By contrast, the inner retina activity and retinal blood flow in light versus dark adaptation are controversial. One of the most popular noninvasive techniques to study light and dark adaptation is laser Doppler flowmetry, but it is limited to either the optic nerve head (ONH), which is dominated by large retinal vessels (distant from sites of increased neural activity), or the fovea, which are void of retinal vessels.

MRI, by contrast, offers depth-resolved information with large field of view. MRI has recently been applied to image anatomical layers,[4–6] relaxation time and diffusion constants,[6–8] blood-oxygenation level dependent (BOLD) responses to physiological[5] and visual[9–11] stimulations, and quantitative blood flow[12,13] of the retinas in animal models. These approaches have been applied to study retinal degeneration,[5,12] diabetic retinopathy,[14] and glaucoma[15] in animal models. More recently, feasibility of anatomical,[16] BOLD,[17] and blood-flow[18,19] MRI of the human retina have also been demonstrated.

Functional manganese-enhanced MRI (MEMRI)[20,21] has also been used to study the retina in animal models.[22] Manganese (Mn) is a calcium analog and an MRI contrast agent. Unlike calcium, once internalized, Mn is trapped intracellularly with a long (hours) half-life. Thus, MEMRI can be used to image calcium-dependent activity[20,21] in a manner similar to the 2-deoxyglucose autoradiography technique, but it can be used to longitudinally study the same animals. Functional MEMRI has several advantages over other functional imaging techniques in animals. First, functional encoding can be done under awake conditions outside the MRI scanner, in contrast to the widely used BOLD fMRI technique, which generally requires animals to be under anesthesia. This is because the activity encoding of functional data can be achieved while the animal is awake and the trapped Mn can be imaged later under anesthesia. Second, MEMRI measures changes in calcium activity, independent of hemodynamic effects, which offers more direct mapping of neural activity.[21] Third, conventional T_1-weighted MRI can be used, in contrast to echo-planar imaging commonly in BOLD fMRI that is susceptible to image distortion and signal dropout.[21] MEMRI, however, has several limitations. Functional MEMRI experiments often require experimental and control groups to be done on different animals because the intracellularly trapped Mn has a long half-life, precluding the use of repeated or real-time paradigms often employed in conventional BOLD fMRI studies. MEMRI is susceptible to intersubject variation and thus, normalization with respect to an external or internal standard is needed for intersubject comparison (including Mn dosing variations). This is because the T_1-weighted MRI often used in MEMRI is a qualitative measure although a quantitative T_1 map can be obtained.[21] MEMRI application is limited to animal models.

In this study, the authors designed a MEMRI protocol to overcome some of the above mentioned limitations and employed this protocol to image functional activities among different layers of the rat retinas during light versus dark adaptation. Light and dark adaptations were carried out on rats

From the [1]Research Imaging Institute and the [2]Departments of Ophthalmology, Radiology, and Physiology, University of Texas Health Science Center, San Antonio, Texas; and the [3]South Texas Veterans Health Care System, San Antonio, Texas.

Supported in part by NIH/NEI Grants R01 EY014211 and EY018855 and a MERIT Award from the Department of Veterans Affairs.

Submitted for publication October 19, 2011; revised February 20 and April 10, 2012; accepted May 29, 2012.

Disclosure: **B.H. De La Garza**, None; **G. Li**, None; **Y.-Y.I. Shih**, None; **T.Q. Duong**, None

Corresponding author: Timothy Q. Duong, Research Imaging Institute, University of Texas Health Science Center at San Antonio, 8403 Floyd Curl Drive, San Antonio, TX 78229; duongt@uthscsa.edu.

in which one eye was covered and the fellow eye was not in the same animals, avoiding interanimal Mn dosing variation. The encoding of light or dark adaptation was achieved in awake conditions and imaged under anesthetized conditions. Two identical radiofrequency transceiver coils (one for each eye) were implemented to allow interleaved MRI acquisitions in the same settings. MEMRI detected contrasts among the inner retina, outer retina, and choroid. Independent confirmation of the vascular layers and boundaries between layers was documented with an intravascular contrast agent. MEMRI detected differential layer-specific calcium-dependent activities between light and dark adaptation.

Materials and Methods

Animal Preparations

Experiments were performed on normal adult Sprague-Dawley rats (250–350 g, $n = 13$) with Institutional Animal Care and Use Committee approval and in accordance with the ARVO Statement for the Use of Animals in Ophthalmic and Vision Research. In group I ($n = 3$), both eyes were light adapted. The animal was anesthetized for intravenous manganese administration (88 mg $MnCl_2 \times 4\ H_2O$/kg bodyweight, via tail vein) an hour. Tail vein infusion was chosen over intraperitoneal injection because a more consistent effective dosage could be delivered and the information was encoded over a more defined duration, although tail vein infusion was comparatively less convenient. The animal was returned to its cage under ambient room light for 5 hours for neural activity encoding under awake conditions.

In group II ($n = 10$), one eye was light adapted and the fellow eye was dark adapted. The animal was briefly anesthetized with 2% isoflurane for placement of an eye patch and an Elizabethan collar to prevent the animal from removing the eye patch. One eye was randomly chosen to be patched for dark adaptation while the fellow eye was not patched for ambient light adaptation. The animal was allowed to recover from anesthesia for 2 hours to ensure dark adaptation before manganese injection.[23] The animal was re-anesthetized for intravenous manganese administration over an hour. The animal was returned to its cage (with one eye remained patched) under ambient room light for 5 hours for Mn activity encoding under awake conditions.

After 5 hours of adaptation, the animals from both groups were prepared for MRI. The animal was anesthetized, intubated, and mechanically ventilated (Harvard Ventilator Model 683; Harvard Apparatus, Holliston, MA) at ~1% isoflurane.[11] In two animals from group I, the tail vein was catheterized for injection of the contrast agent, monocrystalline iron oxide nanoparticles (MION, 5 mg Fe/kg), to confirm peak assignments. After the animal was secured in a MRI-compatible rat stereotaxic headset, atropine eyedrops were applied topically to dilate pupils and to prevent ciliary muscle movements.[11] Lubricating eyedrops (Systane Ultra; Alcon, Fort Worth, TX) were also placed on each eye. For group II, the applications of eyedrops were applied in dim red light with the eye patch removed. The MRI scanner room was kept dark during MRI.

Immediately before MRI, pancuronium bromide (4 mg/kg first dose, followed by 4 mg/kg/hr, IP) was administered to eliminate eye movement.[5,12,24] End-tidal CO_2, rectal temperature, oximetry, and heart rate were continuously monitored and maintained within normal physiological ranges during MRI.

MRI Resonance Imaging

MRI experiments were performed on an 11.7 T/16-cm scanner (Biospec; Bruker, Billerica, MA), and two identical custom-made surface coils with inner diameters of ~7 mm were placed on each eye. Scout images were acquired to plan a single midsagittal slice bisecting the center of the eye and optic nerve for subsequent imaging in order to minimize partial-volume effect due to retinal curvature.[5] MEMRI were acquired using gradient-echo sequence with repetition time = 150 ms, echo time = 5.1 ms, field of view = 7.5 × 7.5 mm, slice thickness = 0.7 mm, 10 repetitions acquired in time series, acquisition matrix = 384 × 384, yielding an in-plane resolution of 20 × 20 μm.

Image Data Analysis

Image analysis was performed using custom-written programs in data analysis software (MATLAB; Math-Works, Natick, MA) as described previously.[5,13] Time-series data were corrected for drift and motion before offline averaging.[5,13] The retinal image was linearized by radially projecting lines perpendicular to the retina. Intensity profiles were obtained over posterior pole of the eye (see Fig. 1). Individual animal intensity profiles were normalized with respect to the vitreous of each eye to account for slight differences in RF coil sensitivity profiles. The vitreous regions-of-interest (ROI) used was placed in the homologous regions of each eye. Full width at half maximum, peak height, and peak separation were determined for the inner retina, outer retina, and choroid. The signal-to-noise ratios of the MRI images were evaluated by taking retina ROIs and a noise region on the images. Reproducibility within animals was evaluated by taking repeated measurements of the peak signal intensities from each of the three "layers" across 10 repeated trials in the same animals. Reproducibility across animals was evaluated by taking standard deviations for each of the three "layers." All data were expressed as mean ± SD. Statistical analyses were performed by paired *t*-tests with Bonferroni adjustment to correct Type I error in multiple comparisons. The significance level was set at $P < 0.05$.

Results

Figure 1 shows the in vivo MEMRI results of two light-adapted eyes from the same animal (group I). The signal-to-noise ratios between the two eyes were overall similar visually. The signal-to-noise ratios in retina ranged from 18:1 to 24:1. The standard deviation of repeated measurements of the peak signal intensities ranged from 2% to 5% across 10 repeated trials in the same animals. MEMRI images showed layer-specific contrasts in the retinas, with alternating bright, dark, and bright bands. The intensity profiles of the bright, dark, and bright peaks were essentially identical between the two eyes. Sclera was dark (lower signal-to-noise ratios) because it had lower water content. The vitreous was dark because its signal was suppressed.

To help to assign retinal layers, the intravascular contrast agent MION was injected (Fig. 2). Comparison of intensity profiles before and after MION showed that peak #1 was attenuated, peak #2 was not attenuated, and peak #3 was markedly attenuated. Peak #1 was assigned as the inner retina (ganglion cell layer [GCL], inner plexiform layer [IPL], inner nuclear layer [INL], and outer plexiform layer [OPL]), which includes the embedded retinal vessels; peak #2, the avascular outer nuclear layer (ONL, inner segment [IS], and outer segment [OS]); and peak #3, the choroid vascular layer. The peak assignments were based on the peaks and thickness observed in previous ex vivo microscopy,[25] histology,[25] and in vivo[5,26] data with confirmation by vascular specific contrast agent.

Figure 3 shows the functional MEMRI of a dark adapted eye and a light adapted eye from the same animal (group II). The intensity profiles of alternating bright, dark, and bright peaks differed between dark and light adapted eyes. The choroid peaks under dark and light adaptation had similar intensity. The outer retina peak in dark had higher intensity relative to light. The inner retina in dark had slightly lower intensity relative to light. Both positive and negative contrasts between light and dark were observed in this animal but not all animals. Figure 4 shows the group-averaged data with normalization to the

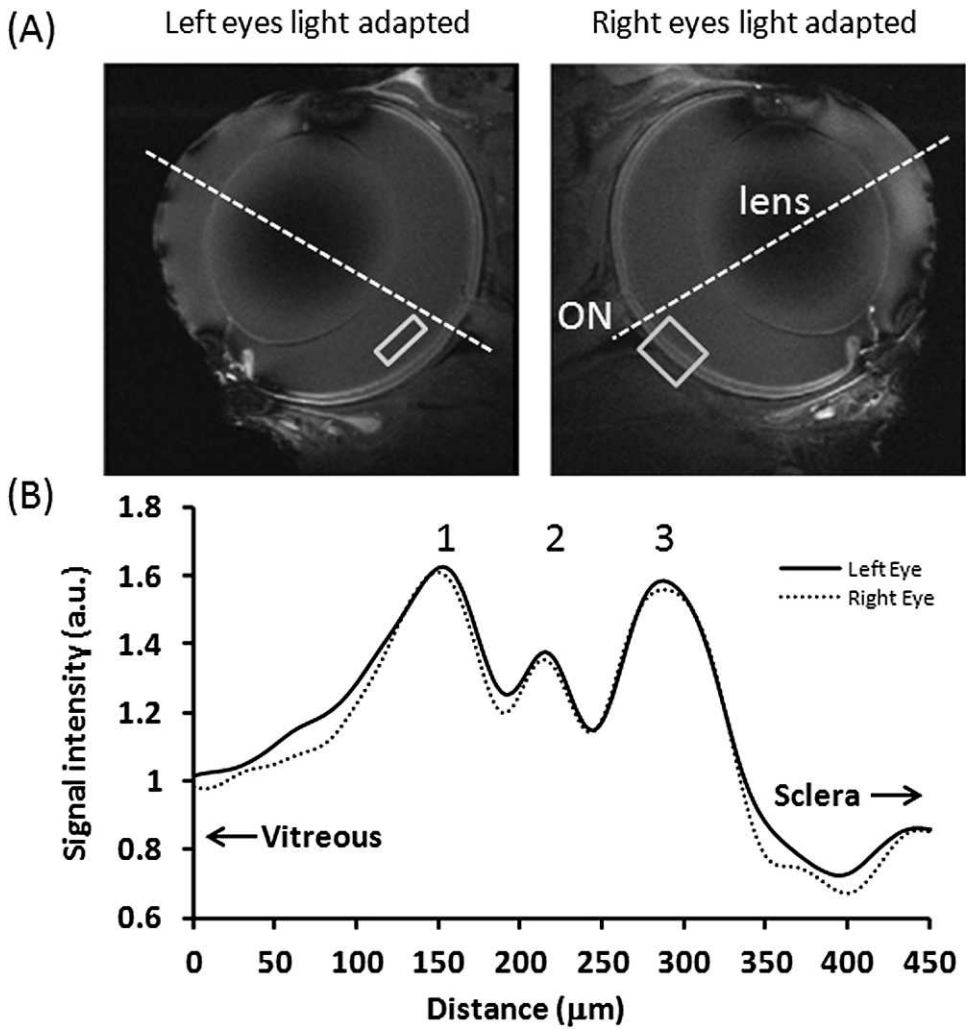

Figure 1. (**A**) MEMRI. (**B**) Intensity profiles across the retinal thickness of two light-adapted eyes from the same animals at $20 \times 20 \times 700$ μm. Normalization was applied with respect to the vitreous. The vitreous ROI shows the typical region used for normalization. The retina ROI shows the typical region where intensity profile is obtained. The *dotted lines* approximate the posterior pole.

vitreous signals. The choroid peaks were iso-intense between dark and light ($P > 0.05$). The outer retina peak under dark was hyperintense relative to light ($P < 0.001$), whereas the inner retina under dark was hypointense relative to light ($P < 0.05$).

The thickness of the inner retina peak was 109 ± 9 μm (mean ± SD), outer retina peak was 65 ± 8 μm, and the choroid peak was 44 ± 6 μm for the eyes exposed to light. The thickness of the inner retina peak was 106 ± 8 μm, outer retina peak was 74 ± 4 μm, and the choroid peak was 40 ± 4 μm for the eye exposed to dark. There were no statistical significances in layer thicknesses between light and dark ($P > 0.05$).

Discussion

This study demonstrates a functional MEMRI protocol for imaging layer-specific calcium activities of the retina in the same animals during light and dark adaptation. Layer-specific functional contrasts in the inner retina, outer retina, and choroid were resolved in vivo. These layer assignments were confirmed by using an intravascular contrast agent. The outer retina had lower MEMRI activity in light compared with dark adaption, whereas the inner retina had higher MEMRI activity in light compared with dark adaption. The choroid MEMRI activity was not statistically different between light and dark adaption. The retinal layer thicknesses were analyzed with confirmation of an intravascular contrast agent.

When both eyes were light adapted (Fig. 1), the images of the two eyes have similar signal-to-noise ratio overall, confirming similar performance of the two radiofrequency coils. The normalized intensity profiles were essentially identical, further confirming the reliability of the approach. The alternating bright, dark, and bright peaks—assigned as the inner retina (GCL, IPL, INL, OPL), outer retina (ONL, IS+OS) and choroid, respectively—were confirmed by using an intravascular contrast agent which changed the signal intensity of the retinal vascular layers (retinal vessels permeated the inner retina) and the choroid bounding the retina, but did not change the signal intensity of the avascular outer retina in between as expected (Fig. 2). These layer assignments are consistent with those reported by Cheng et al.,[5] that employed a different intravascular contrast agent. The thicknesses of the inner retina and outer retina are consistent with those reported by Cheng et al.[5] The choroid thickness herein was slightly thinner than Cheng et al.[5] (inner, outer, and choroid thicknesses were 101 ± 17, 79 ± 11, and 86 ± 10 μm, respectively, at $60 \times 60 \times 500$ μm resolution).[5] This could be

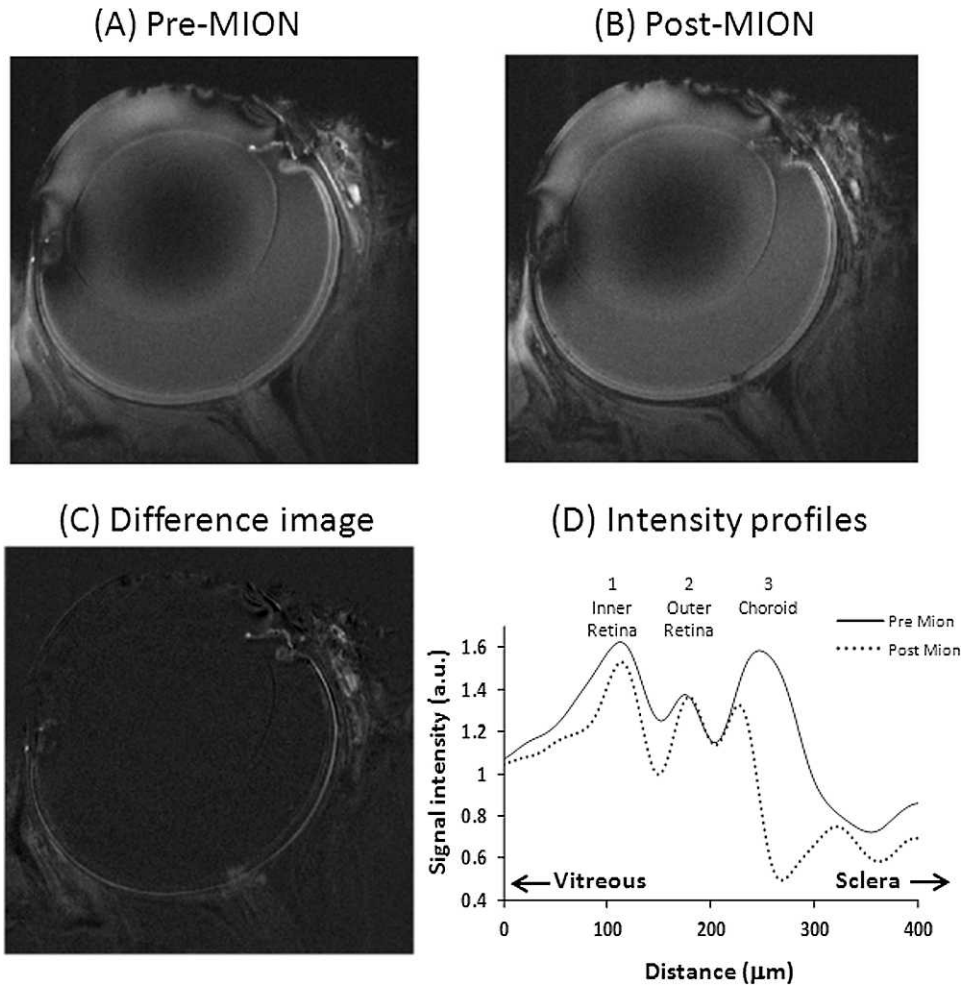

Figure 2. (**A**) MEMRI before. (**B**) After MION injection. (**C**) Difference image. (**D**) Their intensity profiles across the retinal thickness (one animal). Normalization was applied with respect to the vitreous.

due to differences in spatial resolution or regions of the retina analyzed. The study's neural retinal thickness is also in good agreement with the total thickness of the rat neural retina reported using histology,[27,28] ultrasound,[29] and optical coherence tomography.[30,31]

In the outer retina, photoreceptors depolarize in dark and hyperpolarize in light. Depolarization is characterized by a net influx of positive ions, which triggers calcium influx into the intracellular space.[20,21] Such a "dark current" in the outer retina results in a higher metabolic rate in dark than in light.[32] Light adaptation relative to dark adaptation reduced oxygen consumption by 40%, glucose consumption by 44%, and lactate formation by 63% in the pig outer retina.[33] Similarly, light adaptation reduced oxygen consumption by 50%,[34] in the cat outer retina.[35] There is consensus in the literature that functional activities in the outer retina, as measured by different techniques, are higher in the dark than in light. Calcium-dependent MEMRI activities are thus expected to be higher in dark (depolarized state) relative to light (hyperpolarized state) (Fig. 3).

In the inner retina, the literature data are controversial. No change, decrease, and increase activity in light compared with dark have been reported in the inner retina. Activities of the ON and OFF bipolar cells could conceivably balance out irrespectively of light and dark adaptation, potentially resulting in no net activity difference in the inner retina. Arteriovenous sampling from an artery and a plexus on the optic nerve which drains blood from the retina showed no significant differences in glucose and oxygen consumption in the inner retina between light and dark in pig eyes.[36] This method, however, may not have sufficient sensitivity. Oxygen-electrode studies also found no changes in inner retina oxygen consumption between light and dark adaptation.[37,38] Human retinal blood flow velocity has been reported to be lower in light compared with dark as measured by laser Doppler velocimetry.[39]

There are considerably more studies that reported higher activities in light compared with dark in the inner retina. Human retinal blood flow, which is tightly coupled to increased neural activity in the retinal vessels, has been reported to increase (~37%) from dark to light.[3] Fluorescent microsphere study in rats also showed that retinal BF was higher in light than in dark[40] where the experimental conditions were essentially identical to the current MEMRI study except that the fluorescent microsphere study was done under anesthesia. Oxygen-electrode measurements showed that, under light-adapted conditions, oxygen uptake in the inner retina is higher compared with dark-adapted conditions.[41] In the current study, MEMRI activity of the inner retina was found to be higher in light compared with dark. In short, there is accumulated evidence that neural activity is higher in light compared to dark. The discrepancies with some studies could be due to differences in species, experimental conditions, and luminance of light adaptation. It is also possible that different metrics of "neural" activities (such as calcium activity,

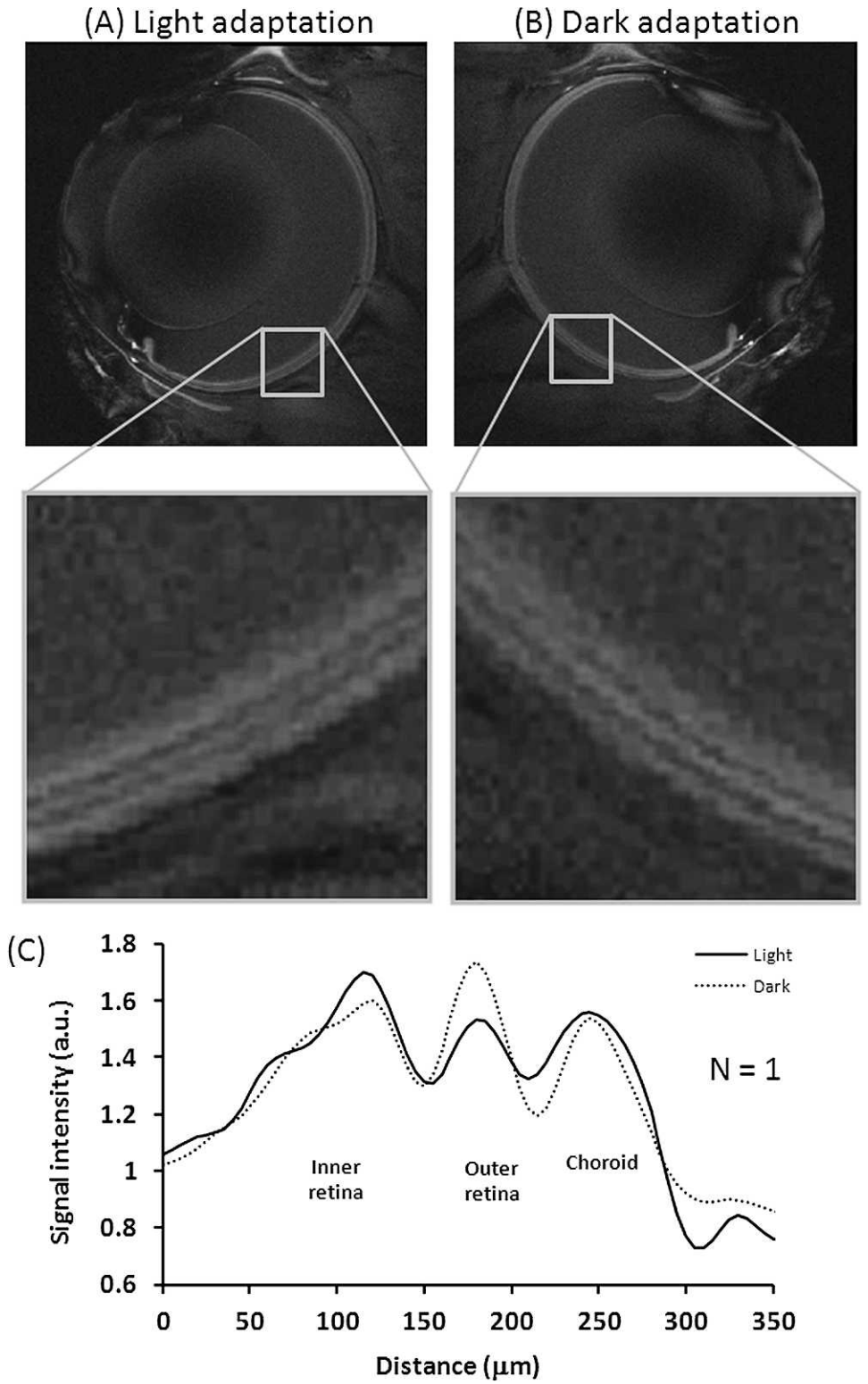

Figure 3. MEMRI images. (**A**) Light-adapted eye. (**B**) Dark-adapted eye. (**C**) Their intensity profiles across the retinal thickness from the same animal at $20 \times 20 \times 700$ µm. Normalization was applied with respect to the vitreous.

blood flow, glucose consumption, or oxygen consumption) may indeed differ as they measure different aspects of increased functional activities.

In the choroid, no significant difference in MEMRI activities was found between light and dark adaptation. The entire choroid layer appeared to be enhanced by Mn. Manganese ions are likely localized in the intracellular space of the retinal pigment epithelium and the endothelial cells outlining choroidal vessels, which are unlikely to differ between light and dark conditions. Choroid BF is generally unresponsive to visual stimulation, and light and dark adaptation as detected by using laser Doppler flowmetry techniques in humans,[42]

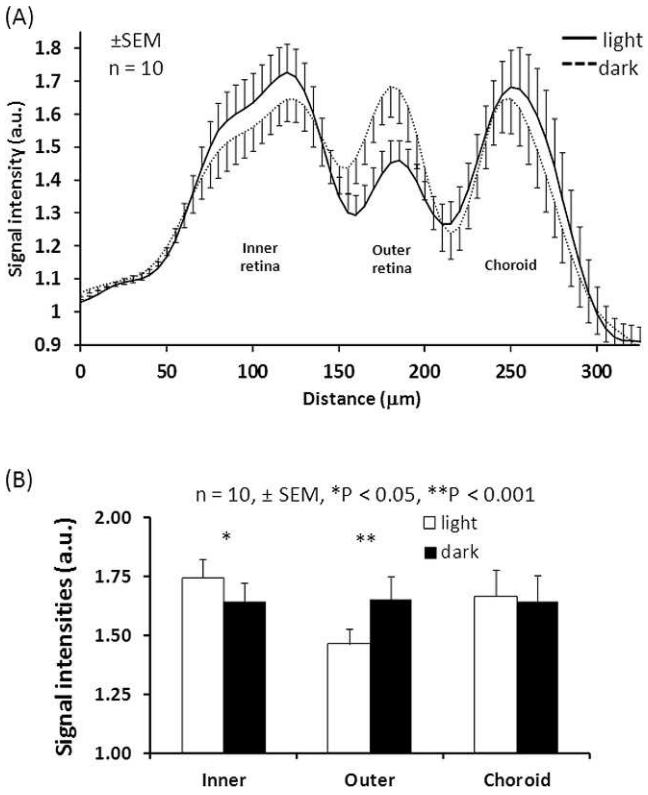

Figure 4. **(A)** MEMRI group-averaged intensity profiles from the dark- and light-adapted eyes (mean ± SEM, $n = 10$) with normalization to the vitreous signals. **(B)** Peak height comparisons of inner retina, outer retina, and choroid (mean ± SEM, $n = 10$, $^{*}P < 0.05$, $^{**}P < 0.001$).

although exception has been noted.[3] Others have also suggested that choroid is not regulated by local metabolic controls.[43] Similarly, functional MRI using a blood-volume contrast agent also found that choroid blood volume did not differ significantly during graded luminance, flicker frequency, and color in rats.[10] A recent fluorescent microsphere study found choroidal blood flow in rats was not statistically different between light and dark.[40] These blood-volume functional MRI and fluorescent microsphere studies were done under similar experimental conditions (except under anesthesia) as the current MEMRI study. There are no direct innervation between the photoreceptors and choroidal arterioles. Basal choroid BF is high, which appears sufficient to maintain adequate oxygen supplies irrespective of light or dark adaptation. High choroid BF has also been suggested to be necessary to dissipate heat.[44,45] In short, the MEMRI findings of the current study are in good agreement with the predominant literatures that the choroid does not change significantly due to changing luminance.

Current study results differed from those of Berkowitz's MEMRI findings.[22,46] Berkowitz et al. assigned the outer MEMRI band of the retina to include the ONL, IS, OS, and choroid, and they found this band to have higher intensity under dark than light. The present study overcame methodological challenges to unambiguously resolve the avascular layer (ONL, IS+OS) from the choroid. Independent confirmation of the vascular layers and boundaries between layers was documented with an intravascular contrast agent. Another difference is that they did not detect MEMRI activity differences between light and dark adaptation in the inner retina, in contrast to the current study. These differences in findings could be due to differences in image spatial resolution and/or different normalization used. Luminance levels, species/strain, and route of Mn administration (IV versus IP) between the two studies are unlikely to contribute to these discrepancies.

Other functional imaging techniques of the retina include intrinsic optical imaging,[47] laser Doppler flowmetry,[42] laser speckle imaging,[48,49] and depth-resolved functional optical coherence tomography.[50,51] Intrinsic optical imaging measures reflectance associated with visual stimulation, albeit without laminar resolution. Laser Doppler flowmetry and laser speckle imaging measured blood flow changes associated with visual stimulation, albeit without laminar resolution. Functional OCT offers remarkable spatial resolution and it can detect reflectance and blood flow changes associated with visual stimuli from single vessels and photoreceptors. Comparisons of different functional imaging techniques of the retina using identical experimental parameters would help to further characterize the metabolic and hemodynamic demands associated with light and dark adaptation.

In conclusion, this study demonstrated high-resolution MEMRI to image layer-specific, calcium-dependent functional activities in the inner retina, outer retina, and choroid in vivo during light and dark adaptation in animal models. This approach can be used to probe retinal dysfunction in diseased states. Future studies need to improve MEMRI spatial resolution to visualize additional major layers of the retina and apply MEMRI to investigate retinal diseases, such as diabetic retinopathy, glaucoma and retinal degeneration in animal models. Improvement in image acquisition speed and signal-to-noise ratio are expected with phase-array acquisitions in which both eyes could be imaged simultaneously while leveraging the highly sensitive small detectors.

References

1. Riva CE, Logean E, Falsini B. Visually evoked hemodynamical response and assessment of neurovascular coupling in the optic nerve and retina. *Progress Retinal Eye Res*. 2005;24: 183–215.
2. Morimoto N. Study on choroidal blood flow at dark and light adaptation. 1. Choroidal blood flow at dark adaptation. *Nihon Ganka Gakkai Zasshi*. 1989;93:790–795.
3. Longo A, Geiser M, Riva CE. Subfoveal choroidal blood flow in response to light-dark exposure. *Invest Ophthalmol Vis Sci*. 2000;41:2678–2683.
4. Muir ER, Duong TQ. Layer-specific functional and anatomical MRI of the retina with passband balanced SSFP. *Magn Reson Med*. 2011;66:1416–1421.
5. Cheng H, Nair G, Walker TA, et al. Structural and functional MRI reveals multiple retinal layers. *Proc Natl Acad Sci U S A*. 2006;103:17525–17530.
6. Shen Q, Cheng H, Pardue MT, et al. Magnetic resonance imaging of tissue and vascular layers in the cat retina. *J Magn Reson Imaging*. 2006;23:465–472.
7. Nair G, Shen Q, Duong TQ. Relaxation time constants and apparent diffusion coefficients of rat retina at 7 tesla. *Int J Imaging Syst Technol*. 2010;20:126–130.
8. Chen J, Wang Q, Zhang H, et al. In vivo quantification of T(1), T(2), and apparent diffusion coefficient in the mouse retina at 11.74T. *Magn Reson Med*. 2008;59:731–738.
9. Duong TQ, Ngan S-C, Ugurbil K, Kim S-G. Functional magnetic resonance imaging of the retina. *Invest Ophthalmol Vis Sci*. 2002;43:1176–1181.
10. Shih YY, De La Garza BH, Muir ER, et al. Lamina-specific functional MRI of retinal and choroidal responses to visual stimuli. *Invest Ophthalmol Vis Sci*. 2011;52:5303–5310.
11. De La Garza BH, Muir ER, Li G, Shih YY, Duong TQ. Blood oxygenation level-dependent (BOLD) functional MRI of visual

stimulation in the rat retina at 11.7 T. *NMR Biomed*. 2011;24:188–193.

12. Li Y, Cheng H, Shen Q, et al. Blood-flow magnetic resonance imaging of retinal degeneration. *Invest Ophthalmol Vis Sci*. 2009;50:1824–1830.
13. Muir ER, Duong TQ. MRI of retinal and choroid blood flow with laminar resolution. *NMR Biomed*. 2011;24:216–223.
14. Berkowitz BA, Kowluru RA, Frank RN, Kern TS, Hohman TC, Prakash M. Subnormal retinal oxygenation response precedes diabetic-like retinopathy. *Invest Ophthalmol Vis Sci*. 1999;40:2100–2105.
15. Calkins DJ, Horner PJ, Roberts R, Gradianu M, Berkowitz BA. Manganese-enhanced MRI of the DBA/2J mouse model of hereditary glaucoma. *Invest Ophthalmol Vis Sci*. 2008;49:5083–5088.
16. Zhang Y, San O, Peng Q, et al. Lamina-specific anatomical magnetic resonance imaging of the human retina. *Invest Ophthalmol Vis Sci*. 2011;52:7232–7237.
17. Zhang Y, Peng Q, Kiel JW, Rosende CA, Duong TQ. Magnetic resonance imaging of vascular oxygenation changes during hyperoxia and carbogen challenges in the human retina. *Invest Ophthalmol Vis Sci*. 2011;52:286–291.
18. Peng Q, Zhang Y, Oscar San Emeterio Nateras O, van Osch MJP, Duong TQ. Magnetic resonance imaging of blood flow of the human retina. *Magn Reson Med*. 2011;65:1768–1775.
19. Maleki N, Dai W, Alsop DC. Blood flow quantification of the human retina with MRI. *NMR Biomed*. 2011;24:104–111.
20. Lin Y-J, Koretsky AP. Manganese ion enhances T1-weighted MRI during brain activation: an approach to direct imaging of brain function. *Magn Reson Med*. 1997;38:378–398.
21. Duong TQ, Silva AC, Lee SP, Kim SG. Functional MRI of calcium-dependent synaptic activity: cross correlation with CBF and BOLD measurements. *Magn Reson Med*. 2000;43:383–392.
22. Berkowitz BA, Roberts R, Goebel DJ, Luan H. Noninvasive and simultaneous imaging of layer-specific retinal functional adaptation by manganese-enhanced MRI. *Invest Ophthalmol Vis Sci*. 2006;47:2668–2674.
23. Behn D, Doke A, Racine J, Casanova C, Chemtob S, Lachapelle P. Dark adaptation is faster in pigmented than albino rats. *Doc Ophthalmol*. 2003;106:153–159.
24. Li Y, Cheng H, Duong TQ. Blood-flow magnetic resonance imaging of the retina. *Neuroimage*. 2008;39:1744–1751.
25. De La Garza BH, Muir ER, Shih YY, Duong TQ. 3D magnetic resonance microscopy of the ex vivo retina. *Magn Reson Med*. 2012;67:1154–1158.
26. Nair G, Tanaka Y, Kim M, et al. MRI reveals differential regulation of retinal and choroidal blood volumes in rat retina. *Neuroimage*. 2011;54:1063–1069.
27. Toprak AB, Ozbilgin K, Toprak V, Tuglu I, Guler C. A histological analysis of the protective effect of ischemic preconditioning in the rat retina. *Current Eye Res*. 2002;24:234–239.
28. Joly S, Pernet V, Dorfman AL, Chemtob S, Lachapelle P. Light-induced retinopathy: comparing adult and juvenile rats. *Invest Ophthalmo Vis Sci*. 2006;47:3202–3212.
29. Jolly C, Jeanny JC, Behar-Cohen F, Laugier P, Saied A. High-resolution ultrasonograophy of subretinal structure and assessment of retina degeneration in rat. *Exp Eye Res*. 2005;81:592–601.
30. Thomas BB, Arai S, Ikai Y, et al. Retinal transplants evaluated by optical coherence tomography in photoreceptor degenerate rats. *J Neurosci Methods*. 2006;151:186–193.
31. Sho K, Takahashi K, Fukuchi T, Matsumura M. Quantitative evaluation of ischemia-reperfusion injury by optical coherence tomography in the rat retina. *Jpn J Ophthalmol*. 2005;49:109–113.
32. Riva CE, Grunwald JE, Petrig BL. Reactivity of the human retinal circulation to darkness: a laser Doppler velocimetry study. *Invest Ophthalmol Vis Sci*. 1983;24:737–740.
33. Wang L, Tornquist P, Bill A. Glucose metabolism in pig outer retina in light and darkness. *Acta Physiol Scand*. 1997;160:75–81.
34. Linsenmeier RA. Effects of light and darkness on oxygen distribution and consumption in the cat retina. *J Gen Physiol*. 1986;88:521–542.
35. Wang L, Kondo M, Bill A. Glucose metabolism in cat outer retina. Effects of light and hyperoxia. *Invest Ophthalmol Vis Sci*. 1997;38:48–55.
36. Cringle SJ, Yu DY, Yu PK, Su EN. Intraretinal oxygen consumption in the rat in vivo. *Invest Ophthalmol Vis Sci*. 2002;43:1922–1927.
37. Braun RD, Linsenmeier RA, Goldstick TK. Oxygen consumption in the inner and outer retina of the cat. *Invest Ophthalmol Vis Sci.* 1995;3:542–554.
38. Cringle SJ, Yu DY, Yu PK, Su EN. Intraretinal oxygen consumption in the rat in vivo. *Invest Ophthalmol Vis Sci.* 2002;43:1922–1927.
39. Havelius U, Hansen F, Hindfellt B, Krakau, T. Human ocular vasodynamic changes in light and darkness. *Invest Ophthalmol Vis Sci.* 1999;40:1850–1855.
40. Shih Y-YI, Li G, De La Garza BH, Wang L, Duong TQ. Cross validation of retinal and choroidal blood flow using arterial spin labeling MRI and fluorescent microsphere. In Proceedings from the International Society for Magnetic Resonance in Medicine; May 5-May 11, 2012; Melbourne, Australia. Abstract 2039.
41. Yu D-Y, Cringle SJ. Oxygen distribution and consumption within the retina in vascularised and avascular retinas and in the animal models of retinal disease. *Prog in Retinal and Eye Research*. 2001;20:175–208.
42. Garhofer G, Zawinka C, Resch H, Huemer KH, Dorner GT, Schmetterer L. Diffuse luminance flicker increases blood flow in major retinal arteries and veins. *Vision Res*. 2004;44:833–838.
43. Riva CE, Cranstoun SD, Mann RM, Barnes GE. Local choroidal blood flow in the cat by laser Doppler flowmetry. *Invest Ophthalmol Vis Sci*. 1994;35:608–618.
44. Parver LM. Choroidal blood flow as a heat dissipating mechanism in the macula. *Am J Ophthalmol*. 1980;89:641–646.
45. Parver LM, Auker CR, Carpenter DO, Doyle T. Choroidal blood flow. *Arch Ophthalmol*. 1982;100:1327–1330.
46. Bissig D, Berkowitz BA. Same-session functional assessment of rat retina and brain with manganese-enhanced MRI. *Neuroimage*. 2011;58:749–760.
47. Tsunoda K, Oguchi Y, Hanazono G, Tanifuji M. Mapping cone- and rod-induced retinal responsiveness in macaque retina by optical imaging. *Invest Ophthalmol Vis Sci*. 2004;45:3820–3826.
48. Cheng H, Duong TQ. Simplified laser-speckle-imaging analysis method and its application to retinal blood flow imaging. *Opt Lett*. 2007;32:2188–2190.
49. Cheng H, Yan Y, Duong TQ. Temporal statistical analysis of laser speckle image and its application to retinal blood-flow imaging. *Optics Express*. 2008;16:10214–10219.
50. Srinivasan VJ, Chen Y, Duker JS, Fujimoto JG. In vivo functional imaging of intrinsic scattering changes in the human retina with high-speed ultrahigh resolution OCT. *Opt Express*. 2009;17:3861–3877.
51. Drexler W, Fujimoto JG. State-of-the-art retinal optical coherence tomography. *Prog Retin Eye Res*. 2008;27:45–88.